

Core-Shell Magnetic Mesoporous Silica Microspheres with Small Magnetic Nanoparticle as a Core

Zhouhao Wu, Fang Wang, Ning Wang, Yujiao Li, Cheng-an Tao, Jianfang Wang*

College of Liberal Arts and Science, National University of Defense Technology, Changsha, 410073, China

ABSTRACT:

By the improved Stöber method, a core-shell mesoporous silica microsphere was prepared using Fe_3O_4 nanoparticles with the diameter of nearly 20 nm as the magnetic core, tetraethyl orthosilicate as silica source, polyethylene oxide–polypropylene oxide–polyethylene oxide (P123) and Cetyltrimethylammonium bromide (CTAB) as surfactants, 1,3,5-trimethylbenzene (TMB) as Pore expanding agent. The characterization results show that the morphology is regular, the diameter is about 600 nm, and the mesoporous size is over 8 nm.

Key Words: Magnetic mesoporous silica nanoparticles, Core-shell structure, Stöber method

Date of Submission: 25-09-2020

Date of Acceptance: 07-10-2020

I. INTRODUCTION

Magnetic mesoporous silica microspheres (MMSMs) is a kind of mesoporous materials based on silica, which is generally composed of magnetic core, protective layer and mesoporous layer. This material has the advantages of traditional silica-based mesoporous materials, such as high porosity, high specific surface area, low toxicity, good biocompatibility, and easy to functionalization, as well as preferable magnetic properties of magnetic nano materials [1-2]. Compared with other magnetic mesoporous microspheres coated with organic compounds, silica is more stable under acidic conditions, has better anti-redox properties, and can effectively protect the magnetic cores [3]. Owing to these advantages, MMSMs are widely used in chemical industry, environmental science, life science, and many other fields, such as catalyst carrier [4-5], sewage treatment [6-8], DNA separation, drug carrier, etc. [9-12]. In 2004, Wu et al. [13] reported the preparation of MMSMs for the first time, but the size and shape were not regular enough. After more than ten years of development, synthesis methods of MMSMs are becoming more and more diversified. For the preparation of nano-magnetic nuclei, there are mainly coprecipitation method, hydrothermal method, solvothermal method, micro-emulsion method, pyrolytic carbonyl precursor method, et al. Coating of silica can be achieved by sol-gel method or reversed-phase microemulsion method. While surfactant removal is mainly by calcination or solvent extraction. For the MMSMs with different morphology and pore size, one or more of the cationic or non-ionic surfactants

are usually used, and pore-enlarging agents can be added when necessary [14-15].

In practical application, in order to better realize the enrichment and recovery of MMSMs and improve the use efficiency, the size of MMSMs should be greater than $0.5\mu\text{m}$, and Fe_3O_4 nanoparticles with a diameter over 100 nm are often used as magnetic core. The size of nano Fe_3O_4 prepared by co-precipitation method is generally small, and the cost is less than 1 % of Fe_3O_4 with a diameter greater than 100 nm. However, it is difficult to prepare MMSMs with regular morphology and diameter greater than $0.5\mu\text{m}$ utilizing such small size Fe_3O_4 nanoparticle as magnetic core, and there are few reports about it. Cetyltrimethylammonium bromide (CTAB) is often used in the preparation of mesoporous materials. However, due to the size of its micelles, the pore size of the prepared mesoporous material is very small and generally no more than 4 nm. As a triblock copolymer, P123 has a larger micelle size, but its first critical micelle concentration (CMC) is smaller, which makes the mesoporous layer tend to be lamellar in the preparation process. Too small hole and non spherical structure make it have great limitation in practical use.

In this study, a core-shell mesoporous silica microsphere was prepared by the improved Stöber method [16] and characterized, and Fe_3O_4 nanoparticles with the diameter of nearly 20 nm was used as the magnetic core, tetraethyl orthosilicate (TEOS) as silica source, P123 and CTAB as surfactants, 1,3,5-trimethylbenzene (TMB) as Pore expanding agent.

II. MATERIALS AND METHODS

2.1. Materials and Instruments

Fe_3O_4 nanoparticles dispersion (10-30 nm, 25wt%, water medium), polyethylene oxide-polypropylene oxide-polyethylene oxide (P123, average molecular weight about 5800). Cetyltrimethylammonium bromide (CTAB), tetraethyl orthosilicate (TEOS), 1,3,5-trimethylbenzene (TMB) were analytically pure.

The structure was studied by a Fourier

2.2 Methods

The preparation process of MMSMs is shown in Figure 1:

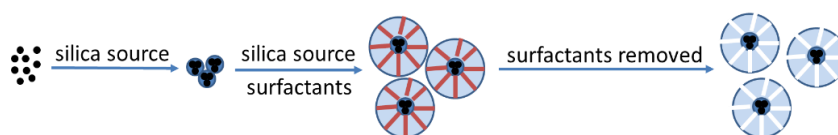


Figure 1 Schematic of the preparation process of MMSMs

2.2.1 Preparation of protective layer

Absolute ethanol (400 mL), deionized water (100 mL) and concentrated ammonia water (about 25~28wt%, 4 mL) were added into the three-neck flask, and Fe_3O_4 nanoparticles dispersion (2 mL) was added under mechanical stirring. After continuous stirring for 15 min, TEOS (5.8 mL) was added within 2 min. After stirring for more than 12 hours, the solid materials were separated by magnet, washed with ethanol and deionized water, and then dispersed in appropriate amount of ethanol to prepare the dispersion of magnetic microspheres with silica protective layer ($\text{Fe}_3\text{O}_4@SiO_2$).

2.2.2 Preparation of mesoporous layer

Transfer $\text{Fe}_3\text{O}_4@SiO_2$ to a three neck flask and add polyether P123 (0.79g), then add CTAB and TMB in sequence according to $m_{P123}:m_{CTAB}:m_{TMB} = 0.79:0.16:0.24$, $0.79:0.16:0.32$, $0.79:0.24:0.24$ (recorded as a, b, c, respectively). After that, it was dissolved and dispersed with hydrochloric acid (1.5M, 200 mL). The reactor was placed at 35 °C and mechanically stirred at a stirring speed of 450 r/min. TEOS (0.92 mL) was added within 1 min. After stirring for 1 h, the temperature was raised to 75 °C, the stirring speed was changed to 700 r/min. After stirring for more than 12 hours, the temperature was raised to 125 °C, and the stirring was continued for 4 h. Then, the solid materials were separated by magnet, washed with ethanol and deionized water, dried at 80 °C, and calcined in resistance furnace (550 °C) for 6h. Three kinds of MMSMs (MMSMs -a, MMSMs -b

and MMSMs -c respectively) were prepared.

III. RESULTS AND DISCUSSION

3.1 Characterization of $\text{Fe}_3\text{O}_4@SiO_2$

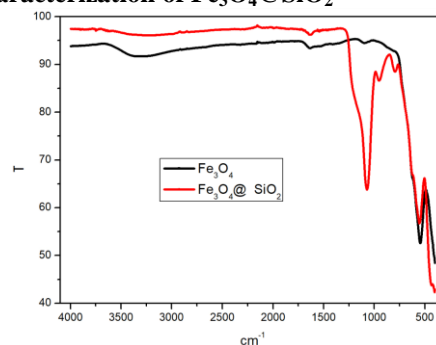


Figure 2 Infrared spectra of Fe_3O_4 nanoparticles and $\text{Fe}_3\text{O}_4@SiO_2$

The infrared spectra of Fe_3O_4 nanoparticles and $\text{Fe}_3\text{O}_4@SiO_2$ are shown in Fig. 2. The peak at 555cm^{-1} is the infrared characteristic absorption peak of Fe_3O_4 . The strong absorption peak at 1073cm^{-1} is caused by the antisymmetric stretching vibration of Si-O-Si bond. The absorption peak at 794cm^{-1} is caused by the symmetric stretching vibration of Si-O-Si bond. The shoulder peak at 436cm^{-1} may be caused by the bending vibration of Si-O bond. The absorption peak at 953cm^{-1} may be caused by the asymmetry of local defects in SiO_2 skeleton, or the characteristic absorption of stretching vibration of Si-O bond.

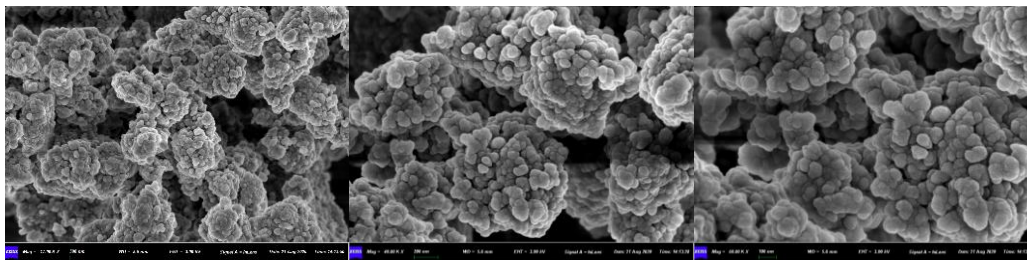


Figure 3 SEM images of Fe₃O₄@SiO₂ indifferent magnification

The SEM of Fe₃O₄@SiO₂ is shown in Fig. 3. Serious agglomeration and irregular morphology appear after coating the surface of small-sized Fe₃O₄ nanoparticles with silica, which size is about 70nm.

Therefore, the synthesis of regular MMSMs needs to choose an appropriate method for mesoporous layer preparation.

3.2 Characterization of MMSMs

3.2.1 Nitrogen adsorption and desorption of MMSMs

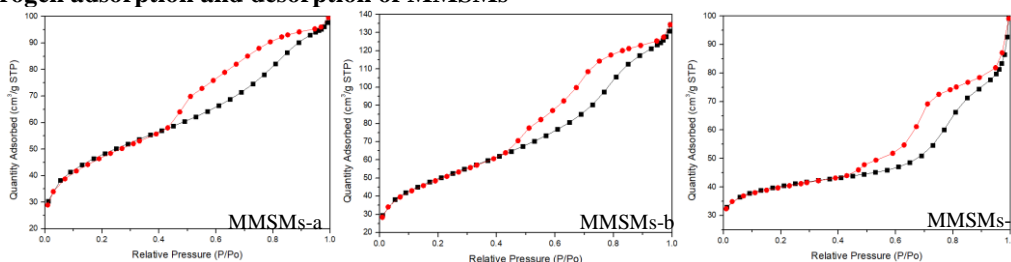


Figure 4 Adsorption and desorption isotherms of MMSMs

The adsorption and desorption isotherms of the three prepared MMSMs (MMSMs-a, MMSMs-b, MMSMs-c) are shown in Fig. 4. Hysteresis loops appear in all the three, indicating that there are mesoporous structures. BET specific surface areas are 169.5 m²/g, 177.9 m²/g and 160.3 m²/g respectively. According to the definition given by the

International Union of theoretical and Applied Chemistry (IUPAC), there are some spherical particles with uniform distribution and slit structure formed between particles, because the adsorption isotherms are all close to type IV and the hysteresis loops are close to the mixed type of H1 and H4.

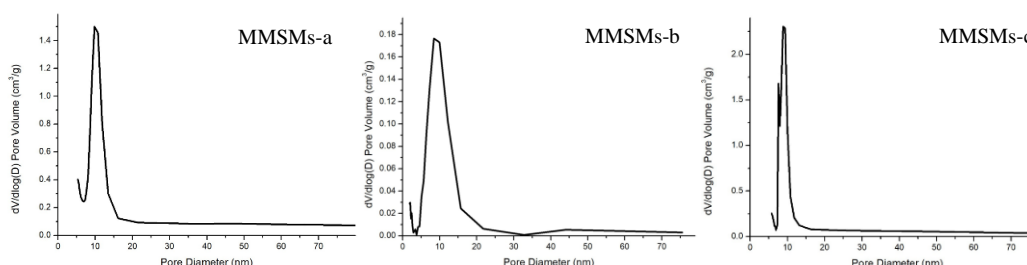


Figure 5 BJH pore size distribution of MMSMs

Fig. 5 shows that the most probable pore sizes of the three MMSMs are 9.1 nm, 10.2 nm and 8.8 nm, respectively. Compared with MMSMs-a, the pore size of MMSMs-b increase slightly and the pore size distribution range also increases with the amount of TMB increasing, which does not meet the

preparation expectation. With the amount of CTAB increasing, the pore size of MMSMs-c is slightly reduced much compared with MMSMs-a, but it is still above 8 nm, and the pore size distribution range does not change much.

3.2.2 SEM Images of MMSMs-a and MMSMs-c

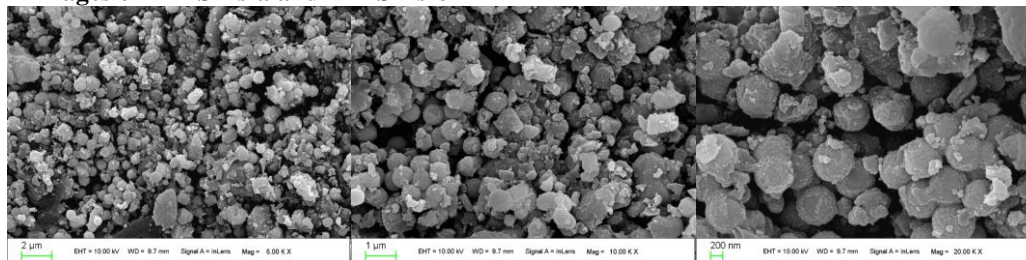


Figure 6 SEM images of MMSMs-a in different magnification

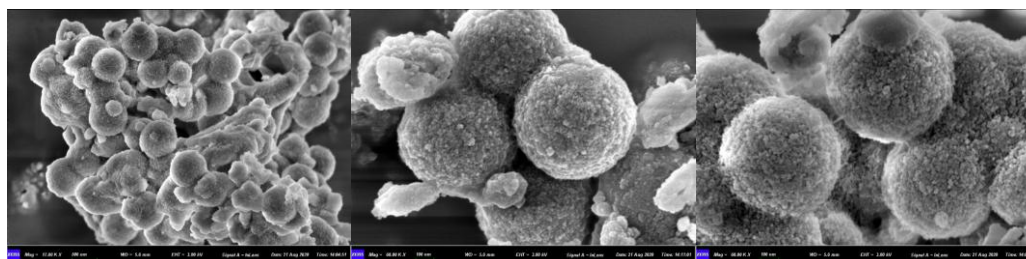


Figure 7 SEM images of MMSMs-c in different magnification

The SEM images of MMSMs-a and MMSMs-c are shown in Fig. 6 and Fig. 7, respectively. It can be found that the spheroidization of MMSMs-a is slightly poor, and there are more flake or irregular shaped nanoparticles in MMSMs prepared with less CTAB. On the other hand, the spheroidization of MMSMs-c is better, the size of the ball is uniform, and the particle size is about 600 nm. The reason may be that the critical micelle concentration of polyether P123 is different from that of CTAB, and different aggregation micelles are produced and different templates are formed by changing the ratio between them. It indicates that the mesoporous materials tend to be spherical when the amount of CTAB is increased in a certain proportion. The pore size and particle size of the three kinds of MMSMs are in accordance with the requirements, and MMSMs-c has more concentrated pore size distribution and more regular morphology.

3.2.3 SAXS of MMSMs-c

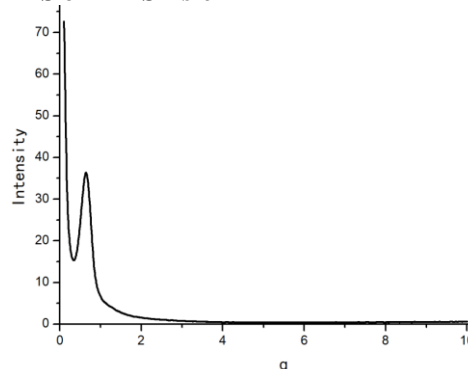


Figure 8 SAXS of MMSMs-c

Fig. 8 shows the Q-I curve of SAXS of MMSMs-c, with $q = 0.7107$ at the extreme point. According to formula (1), (2):

$$q = 4\pi \sin\theta / \lambda \quad (1)$$

$$2d \sin\theta = n\lambda \quad (2)$$

It can be seen that $d = 2\pi/q = 8.84$ nm at the extreme point, which is consistent with the most probable pore sizes measured by BJH method. There is only a single scattering peak, which indicates the existence of mesoporous structure, but the long-range order of the pores is not good.

3.2.4 EDS and mapping analysis of MMSMs-c

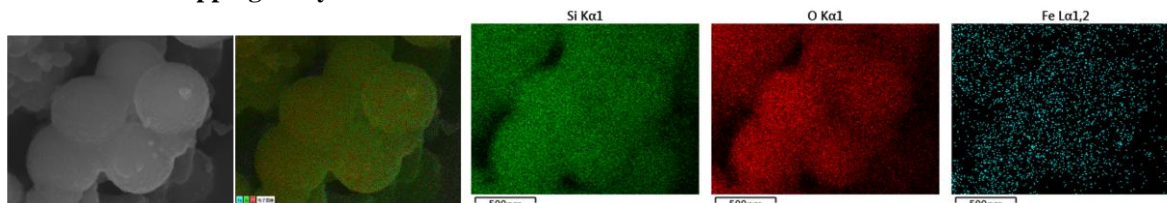


Figure 9 EDS mappings of MMSMs-c

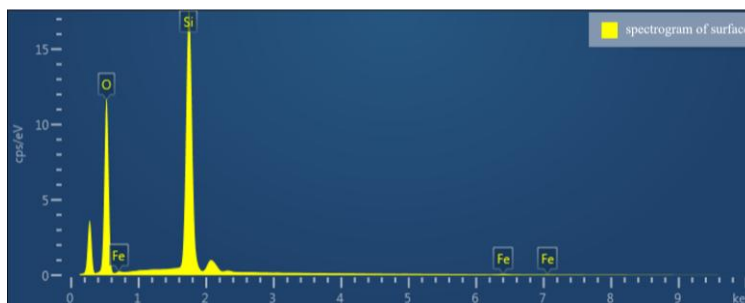


Figure 10 Surface scanning EDS-Mapping of MMSMs-c

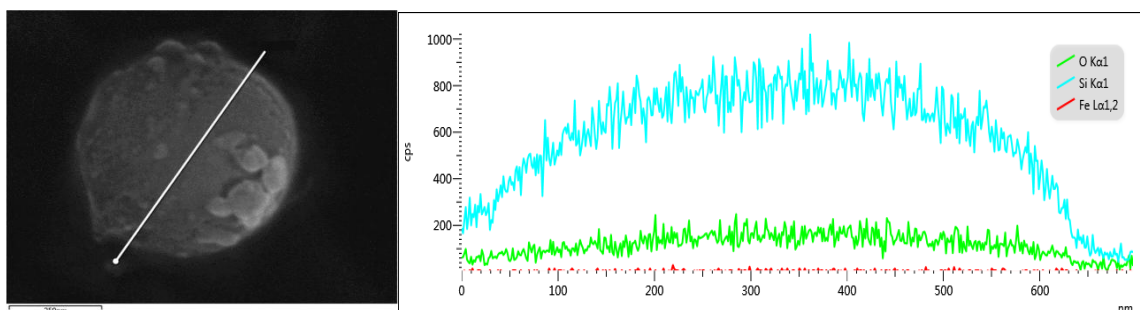


Figure 11 Line scanning EDS-Mapping of MMSMs-c

EDS mappings of MMSMs-c (Fig. 9) show that the microspheres contain O, Si and Fe, and the distribution of O and Si is dense and consistent with the microspheres morphology, while the distribution of Fe is dispersed. According to the surface and line scanning EDS-Mapping of MMSMs-c (Fig. 10, Fig. 11), it can be concluded that the surface of microspheres contains O, Si and no Fe, which indicates that Fe_3O_4 nanoparticles are completely coated by silica and not exposed to the surface of the microspheres. The results show that diameter of the sphere is about 600 nm, which is consistent with the SEM data.

IV. CONCLUSIONS

A kind of core-shell mesoporous silica microspheres with small magnetic Fe_3O_4 nanoparticles core were successfully prepared, whose morphology was regular, with a particle size of about 600 nm and a pore size of more than 8 nm. The effects of CTAB and TMB on the morphology and pore size of MMSMs were studied by comparison experiments. The results show that increasing CTAB dosage in a certain range can make

MMSMs closer to the sphere shape. Meanwhile, the control of TMB dosage can keep the MMSMs with larger pore size without widening the pore distribution range.

Funding

We gratefully acknowledge the financial support of the National Natural Science Foundation of China (21601204).

REFERENCES

- [1]. Zhang Sida, Tao Cheng-an, Wang Jianfang. Progress in Silica-based Electrospun Mesoporous Nanofiber[J]. *Materials Review*, 2016, 30(1): 1-6.
- [2]. Lai Chengyu, Brian G. Trewyn, Dusan M. Jeltinija, et al. A Mesoporous Silica Nanosphere-Based Carrier System with Chemically Removable CdS Nanoparticle Caps for Stimuli-Responsive Controlled Release of Neurotransmitters and Drug Molecules[J]. *Journal of the American Chemical Society*, 2003, 125(15): 4451-4459.
- [3]. Parviz Ashtari, Xiaoxiao He, Kemin Wang,

- Ping Gong. An efficient method for recovery of target ssDNA based on amino-modified silica-coated magnetic nanoparticles[J]. *Talanta*, 2005, 67(3): 548-554.
- [4]. Shaker Masoumeh, Elhamifar Dawood. Core-shell structured magnetic mesoporous silica supported Schiff-base/Pd: an efficacious and reusable nanocatalyst[J]. *New Journal of Chemistry*, 2020, 44(8):3445-3454.
- [5]. Zhao Wanying. On the Controllable Soft-Templating Approach to Mesoporous Silicates[J]. *Chemical Reviews*, 2007, 107(7): 2821-2860.
- [6]. Zhao Dongyuan, Sun Zhenkun, Deng Yonghui, et al. Hierarchically Ordered Macro-/Mesoporous Silica Monolith: Tuning Macropore Entrance Size for Size-Selective Adsorption of Proteins[J]. *Chemistry of Materials*, 2011, 23(8): 2176-2184.
- [7]. Vojoudi Hossein, Badii Alireza, Bahar Shahriyar, et al. A new nano-sorbent for fast and efficient removal of heavy metals from aqueous solutions based on modification of magnetic mesoporous silica nanospheres[J]. *Journal of Magnetism & Magnetic Materials*, 2017, 441: 193-203.
- [8]. Li Dien, Egodawatte Shani Nirasha, Kaplan Daniel I., et al. Sequestration of U(VI) from Acidic, Alkaline and High Ion-Strength Aqueous Media by Functionalized Magnetic Mesoporous Silica Nanoparticles: Capacity and Binding Mechanisms[J]. *Environmental Science & Technology*, 2017, 51(24): 14330-14341.
- [9]. Xiao Haimei, Cai Lei, Chen Shan, Zhang Zhaohui. Magnetic mesoporous silica/graphene oxide based molecularly imprinted polymers for fast selective separation of bovine[J]. *SN Applied Sciences*, 2020, 2(4): 2-12.
- [10]. Hu Xufang, Li Yilin, Miao Aizhu, Deng Chunhui. Dual metal cations coated magnetic mesoporous silica probe for highly selective capture of endogenous phosphopeptides in biological samples[J]. *Microchimica Acta*. 2020, 187(7): 400-410.
- [11]. L. Zhang, S. Z. Qiao, Y. G. Jin, et al. Magnetic Hollow Spheres of Periodic Mesoporous Organosilica and Fe₃O₄ Nanocrystals: Fabrication and Structure Control[J]. *Advanced Materials*, 2008, 20(4): 805-809.
- [12]. Martín-Saavedra, F. M., E. Ruíz-Hernández, A. Boré et al. Magnetic mesoporous silica spheres for hyperthermia therapy[J]. *Acta Biomaterialia*, 2010, 6(12): 4522-4531.
- [13]. Wu Pinggui, Zhu Jianhua, Xu Zhenghe. Template-Assisted Synthesis of Mesoporous Magnetic Nanocomposite Particles[J]. *Advanced Functional Materials*, 2004, 14(4): 345-351.
- [14]. Zuo Bin, Li Wanfang, Wu Xiaoqiang, et al. Recent Advances in the Synthesis, Surface Modifications and Applications of Core-Shell Magnetic Mesoporous Silica Nanospheres[J]. *Chemistry – An Asian Journal*, 2020, 15(8):1248-1265.
- [15]. Bugang Xu, Yonghong Su, Liang Chen, et al. Preparation of mesoporous silica nanoparticles with controlled pore size, particle diameter, morphology, and structure by two-step process of chlorosilane residue[J]. *Ceramics International*, 2018, 44(18): 22241-22248.
- [16]. Kresge C T, Leonowicz M E, Roth W J, et al. Ordered mesoporous molecular sieves synthesized by a liquid-crystal template mechanism[J]. *Nature*, 1992, 359(6397): 710-712.